

Research Article

A Visual Complexity-sensitive DWT Ordering Scheme for Hiding Data in Images

^{1,2}Abdullah M. Iliyasu, ^{1,3}Awad Kh. Al-Asmari, ¹Ahmed S. Salama, ¹Mohammed A. Al-Qodah,

³Mohamed A. Abd Elwahab and ²Phuc Q. Le

¹Salman Bin Abdulaziz University, Al Kharj, Kingdom of Saudi Arabia

²Department of Computational Intelligence and Systems Science, Tokyo Institute of Technology, Japan

³Image and Signal Processing Lab., King Saud University, Kingdom of Saudi Arabia

Abstract: A scheme is proposed to hide data in images based on a prioritized ordering of the content of the host (or cover) image. A watermark embedding process uses the watermark strength to determine the ordering of the 16 regions resulting from the second level Discrete Wavelet Transform (DWT) decomposed content of the host image. To determine the best ordering for hiding the data, various types of image of varying content and, hence, visual complexity were considered, analyzed and ranked in terms of their ability to withstand changes that do not imperil the visual quality (PSNR) of their watermarked versions depending on which an $N \times N$ -sized watermark stream is hidden in the 8 highest ranked sub-bands of the host image. From this perspective, an ordering for images classified as simple, normal and complex images was used to determine a generalized ordering of the DWT decomposed sub-bands of the image. The generalized ordering presented here ascertains that the content of the image and its visual complexity had little effect on an earlier proposed prioritized ordering of the DWT Sub-bands. To validate the veracity of the ordering scheme, 1000 images from the Corel 1000A database, their visual complexity and features were taken into account. The results confirmed that high embedding capacity, appreciable visual quality of watermarked images and complete recovery hidden data are realizable based on the ordering scheme proposed in this study.

Keywords: Data hiding, Discrete Wavelet Transform (DWT), image processing, information security, visual complexity, watermarking

INTRODUCTION

A consequence arising from the recent growth and advancements in the field of digital communication technology is the ease with which information can be produced, exchanged and copied. This has made the need for state-of-the-art algorithms to protect data and multimedia such as text, images, video, sound, etc., against un-authorized copying and tampering both mandatory and de rigueur (Al-Asmari *et al.*, 2012).

Digital watermarking is a technique that proffers a means to guard digital content from illegal copying and manipulation. Over the past few years these digital watermarking techniques have become more advanced, sophisticated and robust. Using a good watermarking technique, it is possible to extract the data embedded in the image at a later stage, or detect its presence in the multimedia element for diverse purposes including copyright protection, access control and broadcast monitoring. Depending on the type of data and applications, or target audience, each watermarking strategy may be designed to enhance at least one of the

properties: capacity, robustness or visual quality (a.k.a. imperceptibility) of the original data. A digital watermark is an unnoticeable signal added to digital data, known as cover content (image, sound, etc., as the case may be), which can possibly be identified at a later stage for identification, authentication or the like. Thus, Digital watermarking can be categorized as image watermarking, video watermarking or audio watermarking depending upon the nature of the cover content. Contemporary digital watermarking schemes chiefly target image and video copyright protection (Wang and Zhao, 2006). Commonly, a digital watermark is a code that is embedded within an image. It plays the role of a digital signature, providing the image with a sense of ownership or authenticity. The primary benefit of watermarking is that the content is not separable from the watermark. Watermarking can be divided into diverse categories in a wide range of ways. It is categorized into non-blind, semi-blind and the blind schemes on the basis of the requirements for watermark extraction or detection (Tao and Eskicioglu, 2004; Weng *et al.*, 2008). In another category, robust watermarking is commonly

designed to resist malicious attacks like scaling, cropping, lossy compression, etc. and is chiefly focused on copyright protection. On the contrary, fragile watermarking is used when the intention is to identify any tiny modification to the original digital content (Weng *et al.*, 2008).

Extensive and recent researches on watermarking techniques for copyright protection have been introduced in the literature including (Kim and Moon, 1999; Elbasi and Eskicioglu, 2006; Makhoghi *et al.*, 2010; Cui and Li, 2011; Wang *et al.*, 2010). Some conventional wavelet watermarking techniques embed the watermark in the components of the first level Discrete Wavelet Transform (DWT). Other techniques, that perform a second level decomposition, obtain the approximation sub-band from the first level decomposition and then decompose it further (Salama *et al.*, 2011).

In Al-Asmari *et al.* (2012), we proposed an embedding process based on an ordering of the DWT decomposed content of the cover images as determined by the watermark strength. The proposal exploits the relationship between the strength of the watermark (or gain factor), K and the imperceptibility of the resulting watermarked images in order to prioritize the ordering of sub-bands of the second order decomposed content of the cover image for the watermark embedding procedure. Using this ordering, the second level DWT decomposed content of the cover image is transformed using the Pixel Value Difference (PVD) in order to embed and recover the hidden data.

Here in, we validate the earlier proposal by considering a larger database comprising of 1000 images from varying categories, content and, hence, the visual complexity of images as perceived by the Human System (HVS) (Le *et al.*, 2012, 2011). The results suggest that notwithstanding the content and complexity of the host images, the proposed ordering of the DWT sub-bands do not change significantly hence, yielding high embedding capacity, good visual quality of watermarked images and efficient watermark recovery.

Succinctly put, the work presented in this study is targeted at improving the embedding capacity and visual quality of watermarked images, while also guaranteeing the complete recovery of the data hidden inside the hitherto watermarked versions of the images.

To accomplish this, our attention is mainly focused on understanding and utilizing the notion of visual complexity of images. Using the Corel 1000A dataset, we generalized the SND visual complexity space (Le *et al.*, 2012, 2011) correlated it with the watermark strength dependent DWT-based watermark embedding in (Al-Asmari *et al.*, 2012). Based on these generalizations, we deduced a relationship between visual complexity of an image and the watermark strength required for effective data hiding. This relationship was used to determine the best ordering to embed the watermark into the second order DWT decomposed content of the cover image using the PVD method.

The proposed ordering scheme enhances the watermark embedding capacity, ensures faithful watermark recovery and guarantees visual fidelity of the watermarked versions of the images. The details of the proposed scheme and its evaluation are presented in subsequent sections of the study.

METHODOLOGY

The role of gain factor in effective hiding of information: In determining the ordering of the sub-bands of the cover image for the watermark embedding, the cover image is decomposed into its first and second tier regions using discrete wavelet transform. The first and second level DWT decomposition of an image is depicted in Fig. 1.

The watermark strength or gain factor, K , was shown, in Salama *et al.* (2011), to have a huge impact of the visual quality of watermarked images and their peak-signal-to-noise-ratios, PSNR, values. Its choice affects the embedding and extraction of hidden data from watermarked images. Figure 2 summarizes the relationship between the gain factor and the fidelity of the watermarked images, denoted by the PSNR values, for the Lena cover image (Salama *et al.*, 2011).

The chart in the figure (Fig. 2) shows the choice of the best value of K for each sub-band of the decomposed image. It indicates the variation in the values of K that would enable the complete recovery of the hidden data. As seen from this figure, the HH band produces the least value of K , hence, it is considered as the best sub-band to hide the watermark logo. In contrast, the LL band would yield the worst watermarked image because it has the highest value of K (as high as 6 in the LL2 sub-band, which is also referred to as the LLLL sub-band).

Consequently, this suggests that the choice of K influences the fidelity (PSNR) of watermarked images as manifested in the chart in Fig. 3 for the same Lena cover image. From this figure we see that the LL2 and HL2, i.e., second level decomposed sub-bands, of the HH band (the HHLL and HHHL sub-bands) have the highest PSNR values (close to 50 dB), while the worst PSNR values are found in the LLLL sub-band. This inverse relationship is further summarized in Fig. 4. The PSNR value decreases as K increases until it reaches its maximum value (at K equal to 20).



Fig. 1: A DWT decomposed image, its 4 bands (LL, HL, LH and HH) and second level sub-bands LL2, HL2, LH2 and HH2

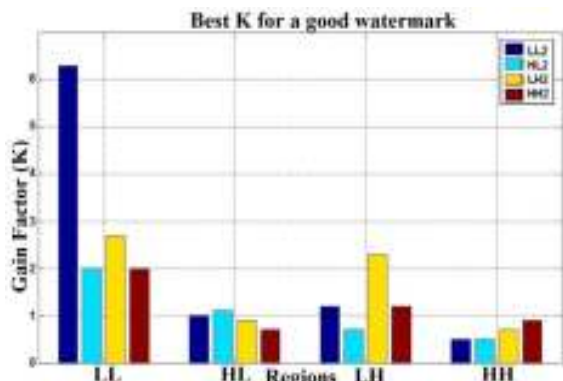


Fig. 2: The best K to recover watermarked Lena image

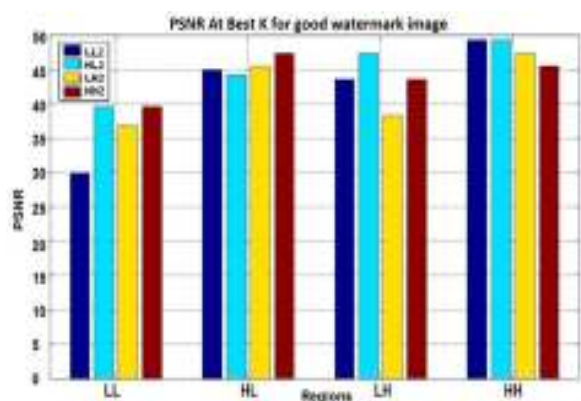


Fig. 3: PSNR at best K to recover a complete watermark signal/logo from the watermarked Lena image

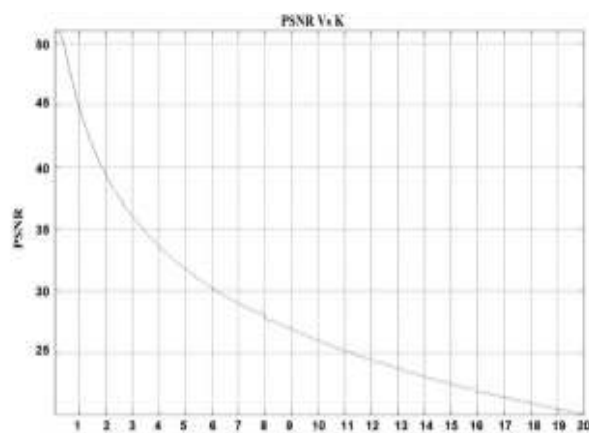


Fig. 4: Variation in PSNR versus gain factor (K) for Lena host image

The foregoing discussions indicate that the least value of K is always most desirable in terms of high embedding and recovery of the data hidden in images. For the Lena image, the least value of K is found at $K = 0.5$, i.e., in the HHLL sub-band. It was also proven in Salama *et al.* (2011) that hiding data in the HHLL sub-band produces high fidelity marked images whose

original content can be completely recovered. As noted earlier, Fig. 4 shows the variation between the watermarked image fidelity (PSNR) and the change in K for the Lena host image as presented in Al-Asmari *et al.* (2011).

In the sequel, we revise the SND space for representing visual complexity and generalize the aforementioned relationship between the choice of best K and the quality (capacity and imperceptibility) for a larger dataset, the Corel 1000A database.

SND space for representing image visual complexity: The evaluation of visual complexity of images is important in revealing the depth of information hidden in the images besides the lower level information pertaining to their colors, brightness and edges. This high level property is useful in many real applications of image processing, such as feature extraction, image watermarking and feature mining (Ilyasu *et al.*, 2013b). Visual complexity has been represented using single features such as quad tree (Yaghmaee and Jamzad, 2005), edge based measurement (Mario *et al.*, 2005), fuzzy measures of entropy (Cardici *et al.*, 2009) and entropy based information (Rigau *et al.*, 2005).

Figure 5 shows a simple case of varying visual complexity of three images (increasing from left to right), one each from the flower, food and building categories of the Corel 1000A database (Griffin *et al.*, 2013).

In Le *et al.* (2011, 2012), a 3D space was used to represent the visual complexity of an image based on its inherent properties, specifically, the structure, noise and diversity hidden in the image itself. This space was appropriately named the SND space because of the features it is built upon.

Figure 6 shows a typical representation of an SND space for a dataset comprising of a few images.

When an SND space is constructed from a set of images, its inherent structure in terms of clusters reveals the visual complexity of images in that space (Le *et al.*, 2011, 2012). In order to identify these clusters, clustering methods such as k-means, fuzzy c-means algorithms can be applied. The labels assigned to the clusters in the SND space express subjective evaluation of the visual complexity of the images by the Human Visual System (HVS). When these labels are assigned to clusters, a new image is automatically categorised by using its visual complexity value to assign to the cluster whose cluster centre is closest to the visual complexity value as demonstrated in the Fig. 7.

The three labels, 'complex', 'normal' and 'simple', are assigned based on the results of the k-means clustering algorithm on three classes. The number of images from the Corel 1000A database that fall in each visual complexity class are summarized in Table 1.



Fig. 5: A few sample images from the Corel 1000A database showing increase in visual complexity from left to right

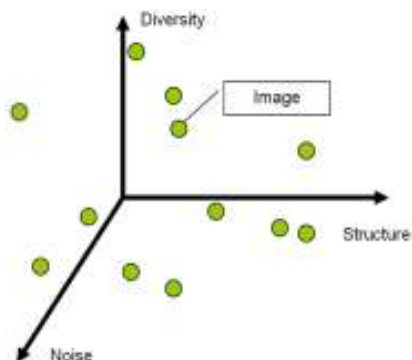


Fig. 6: The SND space

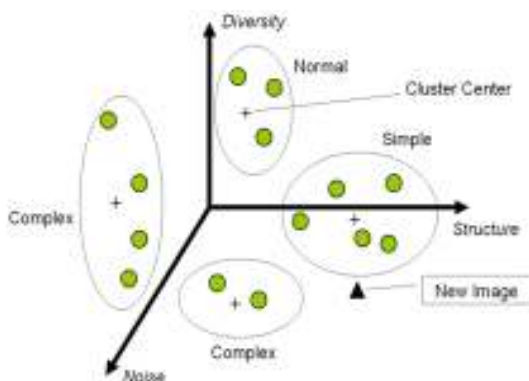


Fig. 7: Clusters in the SND space indicating visual complexity of images

Table 1: Number of images in each cluster using k-means algorithm with 3 clusters on the Corel 1000A dataset

Cluster	Simple	Normal	Complex
No. of images	291	408	301

All images in a cluster are assumed to have the same visual complexity. Meanwhile, the clusters in the SND space and the visual complexity labels express intuitive relations, i.e., an image is considered as complex if it has high structure, noise and diversity; or normal, if it has medium structure, noise and diversity, or simple if the three features are low. Some representative images belonging to the three visual complexity classes for some categories of the Corel 1000A dataset are shown in Fig. 8. As seen there from, images in the simple cluster contained only one



Fig. 8: The sample images for the three visual complexity clusters as extracted from the SND space that was built using the 1000 images in the Corel 1000A dataset



Dinosaurs.061 Buses.02 Mountains.096

Fig. 9: Images at the centre of visual complexity clusters as extracted using the SND space for the Corel 1000A dataset

predominant object such as a human face, or a building and a somewhat flat or continuous background. In similar fashion, images comprising two or three predominant objects and a constant background and those characterized by numerous objects and irregular or discontinuous backgrounds are classified as having normal and complex visual complexity, respectively (Le *et al.*, 2012).

Figure 9 shows images located at the centers of the simple (Dinosaurs.061), normal (Buses.023) and complex (Mountains.096) clusters. We shall use these images as representatives of the simple, normal and complex images. The number of images in each cluster as realised using the SND visual complexity space were earlier summarized in Table 1.

Similar to the earlier discussion on the choice of best K for an image in preceding section and (Al-Asmari *et al.*, 2012), we present in Fig. 10 to 12 the variation of the gain factor for in the LL, LH, HL and HH regions for the representative images that are located at centers of the simple, normal and complex image clusters (i.e., Dinosaurs.061, Buses.023 and Mountains.096, respectively).

In a similar fashion, using the figures in Fig. 10 to 12, we show, in Fig. 13 to 15, the variation in PSNR values in the LL, LH, HL and HH sub-bands for the representative images (i.e., the Dinosaurs.061, Buses.023 and Mountains.096 images) for the simple, normal and complex images.

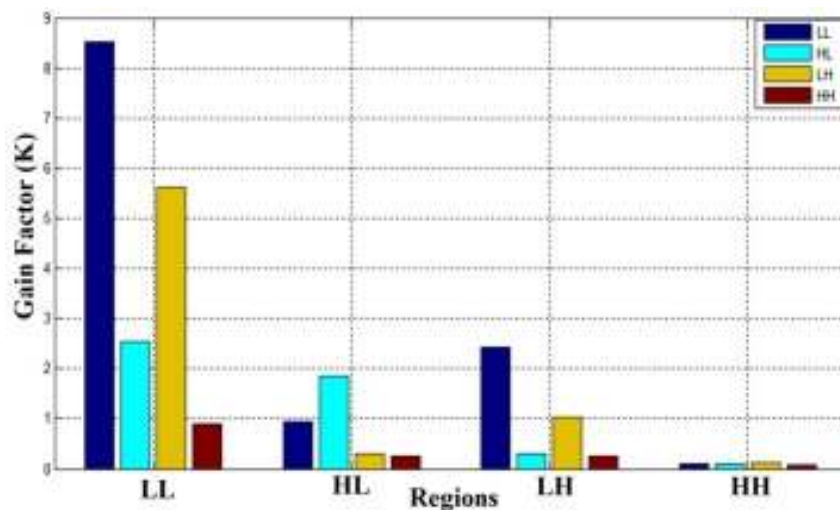


Fig. 10: The best K for the watermarked version of the image at the centre of the 'simple' cluster (Dinosaurs.061)

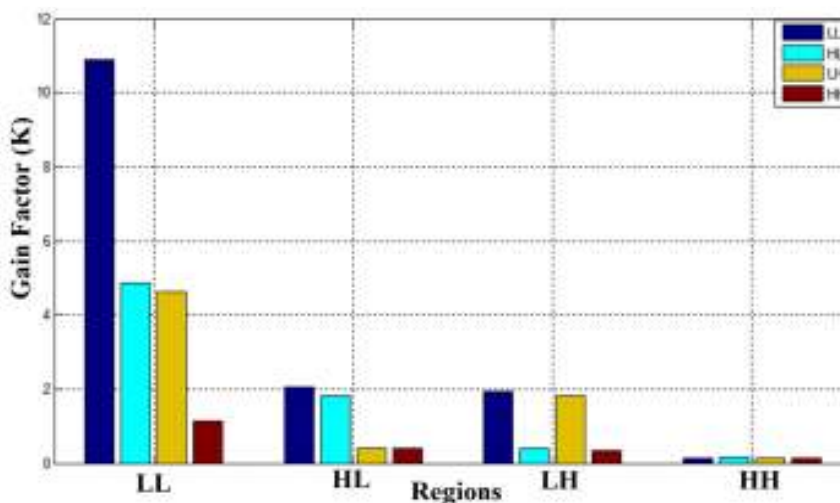


Fig. 11: The best K for the watermarked version of the image at the centre of the 'normal' cluster (Buses.023)

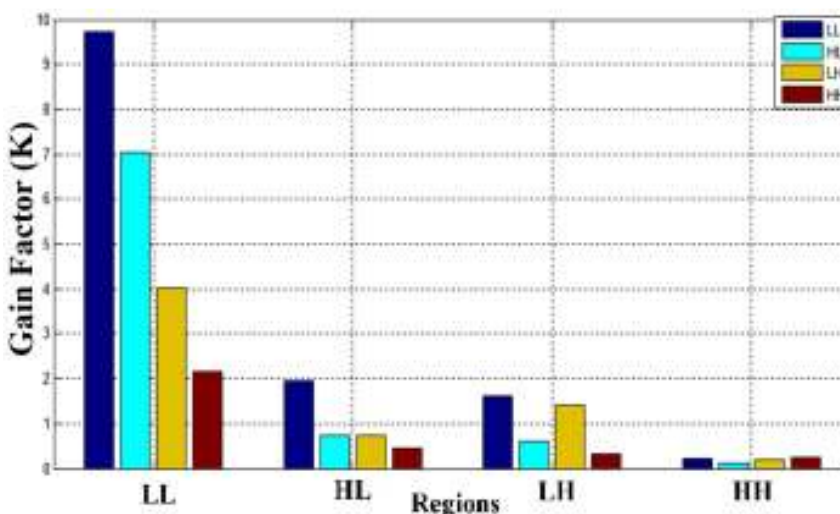


Fig. 12: The best K for the watermarked version of the image at the centre of the 'complex' cluster (Mountains.096)

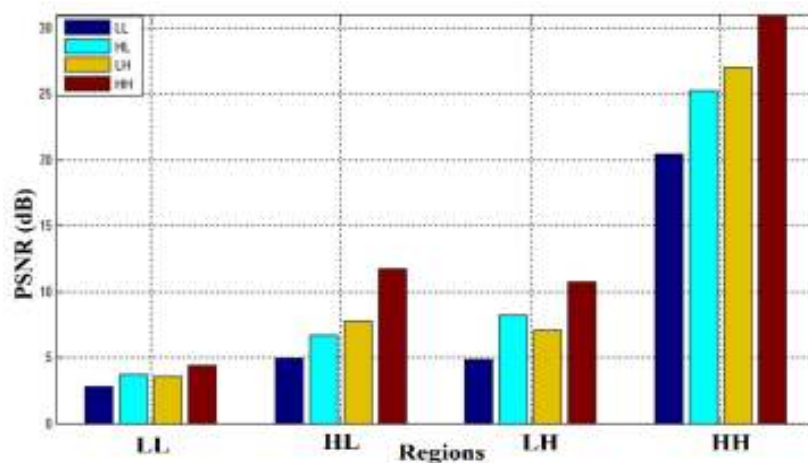


Fig. 13: Variation in PSNR values at different regions of the watermarked logo as recovered from the representative image for 'simple' cluster

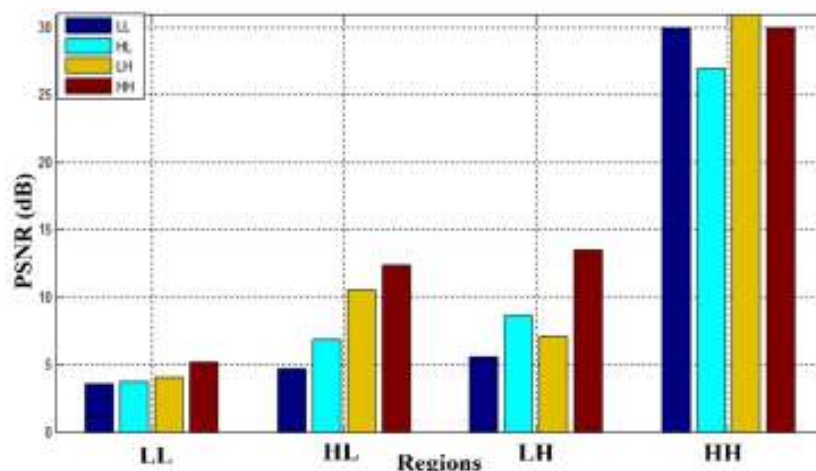


Fig. 14: Variation in PSNR values at different regions of the watermarked logo as recovered from the representative image for 'normal' cluster

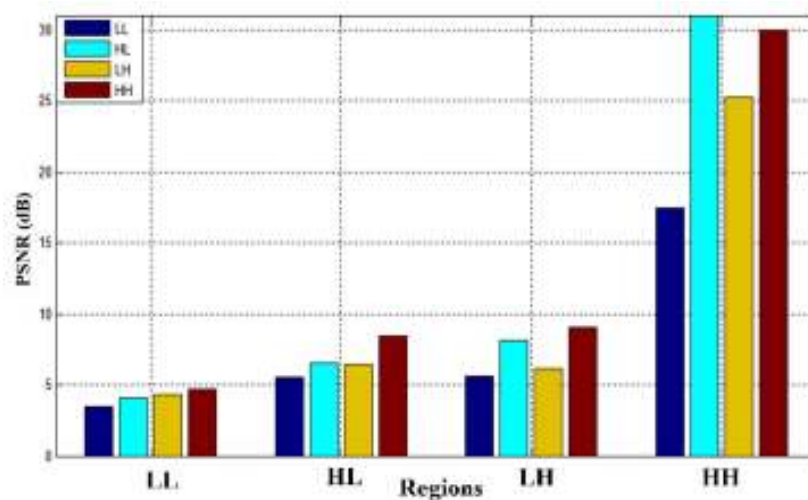


Fig. 15: Variation in PSNR values at different regions of the watermarked logo as recovered from the representative image for 'complex' cluster

Figure 16 shows the ordering of the sub-bands of the DWT decomposed host image representing the simple normal and complex clusters based on the evaluation of the best K.

In this figure, the rightmost letters (LL, HL, HL and HH) indicate the bands of the DWT decomposed host image, while the remaining two letters specify the second level DWT sub-bands as explained earlier in Fig. 1. The indexes 1-12 indicate the priority accorded to each sub-band in the watermark embedding procedure.

The exquisite performance regarding the ease and quality of the embedding and extraction of data presented thus far and in (Al-Asmari *et al.*, 2012) are, however, not generalised for all the sub-bands and therefore there is the need to cull from the 16 sub-bands that make up the best for both the watermark embedding

and extraction. Hence, the need to prioritize the ordering of the sub-bands based on the best choices of K.

In deciding on the orderings in Fig. 16 we ignored the LL region of the DWT decomposed sub-band of the host image because it has been proven to have an adverse effect on the quality of watermarked images and extraction of second level decomposed cover images the ones that are on the quality of watermarked images and extraction of hidden data in already marked images (Al-Asmari *et al.*, 2012; Salama *et al.*, 2011).

The ordering suggested here guarantees high embedding capacity, good visual quality watermarked images and complete recovery of the hidden data, i.e., the watermark.

Figure 17 shows the 10 sample images from the Corel 1000A dataset that were used together with the images located at the centre of the simple, normal and

				12 HLLL	10 HLHL					11 HLLL	10 HLHL					12 HLLL	9 HLHL		
				7 HLLH	6 HLHH					8 HLLH	5 HLHH					8 HLLH	6 HLHH		
11 LHLL	8 LHLH	2 HHLL	4 HHHL					12 LHLL	7 LHLH	4 HHLL	3 HHHL					11 LHLL	7 LHLH	4 HHLL	1 HHHL
9 LHLH	5 LHHH	1 HHHL	3 HHHH					9 LHLH	6 LHHH	2 HHHL	1 HHHH					10 LHLH	5 LHHH	3 HHHL	2 HHHH
Simple cluster				Normal cluster				Complex cluster											

Fig. 16: Ordering for the second order DWT decomposed contents of the representative images in the simple, normal and complex image clusters



Fig. 17: Sample images from the 10 categories of the Corel 1000A dataset

Table 2: Sub-band ordering for the different images in the 10 categories (one for each category) of the Corel 1000A dataset

Order	1	2	3	4	5	6	7	8	9	10	11	12
Africa	HHHH	HHHL	HHHL	HLLL	LHHH	HLHH	LHHL	HLLH	LHLH	HLHL	LHLL	HLLL
Beach							HLLH	LHHL				
Buildings	HHHL		HHHH		HLHH	LHHH	LHHL	HLLH	HLHL	LHLH		
Buses	HHHH		HHHL				HLLH	LHHL	HLLL		HLHL	LHLL
Dinosaurs	HHHL	HHHH					LHHL	HLLH	HLHL		LHLL	HLLL
Elephants	HHHH	HHHL			LHHH	HLHH	LHHL	HLLH				
Flowers					HLHH	LHHH	HLLH	LHHL	HLHL		HLLL	LHLL
Foods							LHHL	HLLH			LHLL	HLLL
Horses	HHHL		HHHH			LHHL	LHHH		LHLH	HLHL		
Mountains	HHHH		HHHL					HLHL	HLLH	LHLH	HLLL	LHLL

LL		12	9
		8	5
11	7	4	3
10	6	2	1

Fig. 18: Generalized DWT sub-band ordering for high performance hiding of data in images

complex clusters in order to determine the best order for each category (of images in the Corel 1000A database) as presented in Table 2.

Using the ordering in Fig. 16 and Table 2, a generalized DWT decomposed sub-band ordering of the images can be obtained irrespective of the content and perceptual complexity of the images. This generalized ordering is presented in Fig. 18.

This ordering generalizes the DWT decomposed ordering (Al-Asmari *et al.*, 2012) for data hiding and recovery and adopting the scheme in Al-Asmari *et al.* (2011), it shall be used in our proposed Pixel Value Difference (PVD)-based watermark embedding and extraction system (Salama *et al.*, 2011) as presented in the next section.

WATERMARK EMBEDDING AND EXTRACTION BASED ON DWT PRIOTISED ORDERING

To accomplish the watermark embedding, the DWT decomposed sub-bands of the cover image were analyzed and ranked in terms of their ability to withstand changes that do not imperil the visual quality (PSNR) of the watermarked image. Based on this analysis, the contents of each pixel in the watermark image are assembled into an 8-bit binary (0-1) bit stream. The Most Significant Bits (MSB) from each pixel are then gathered and hidden in the best wavelet sub-band, the HLLH region, while the Least Significant Bits (LSB) are spread within the HHHH region. Finally, the remainder of the bits from the watermark stream are spread in the remaining 6 sub-bands of the host image. This procedure is depicted in Fig. 19 and discussed at length in Al-Asmari *et al.* (2011).

Figure 20 and 21 present the generalized block diagrams for the data hiding embedding and recovery that combine to make up the proposed scheme as presented in Al-Asmari *et al.* (2011), wherefrom further discussions can be sought.

To extract the watermark image, the 8 highest ranked wavelet sub-bands were decomposed from the watermarked image then the reverse PVD method was used to extract 8 streams of bits from each sub-band.

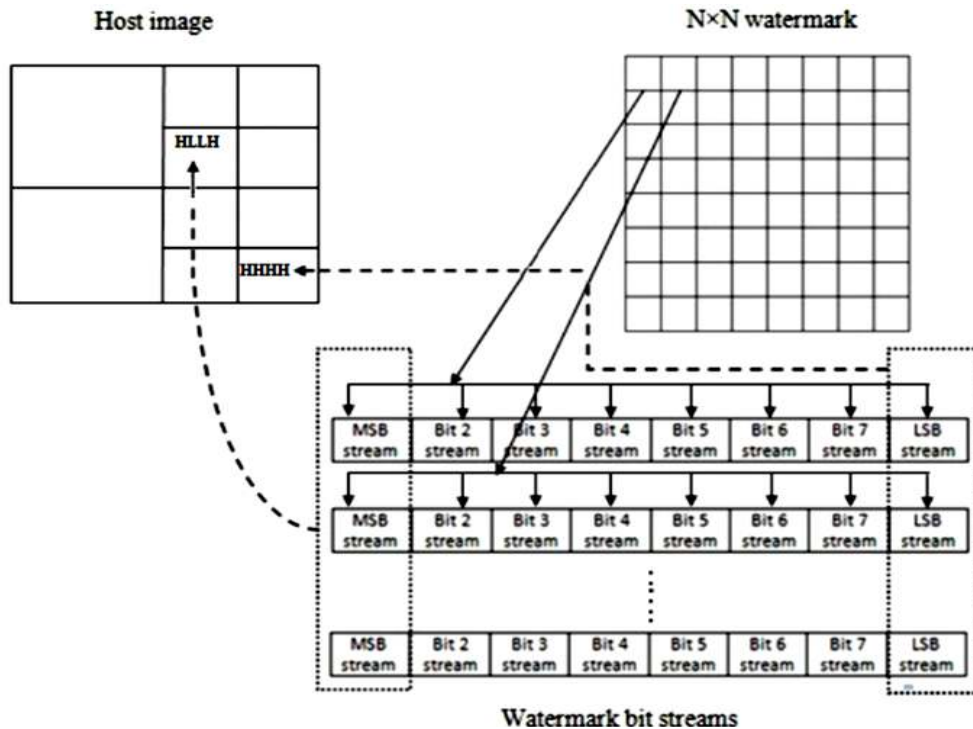


Fig. 19: Watermark bit stream embedding on host image for the representative image located at the centre of the 'simple' cluster (Dinosaurs.061)

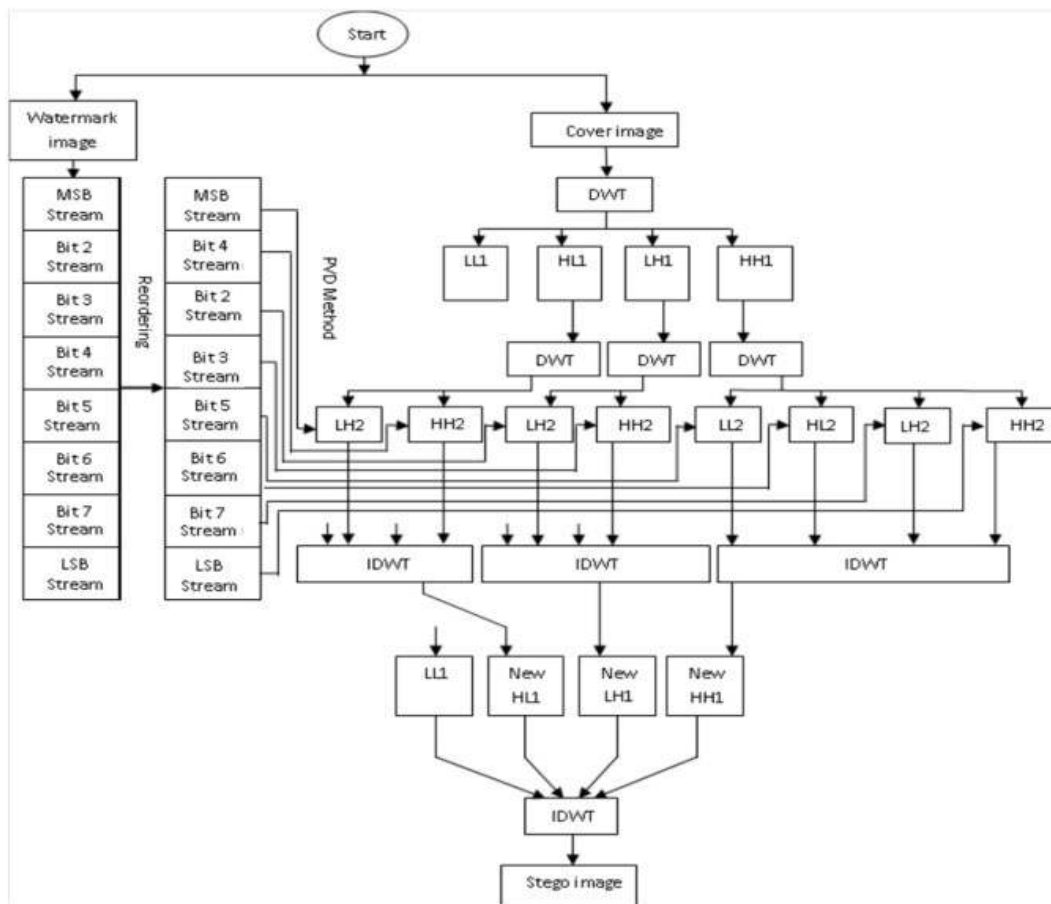


Fig. 20: The watermark embedding procedure (Al-Asmari *et al.*, 2011)

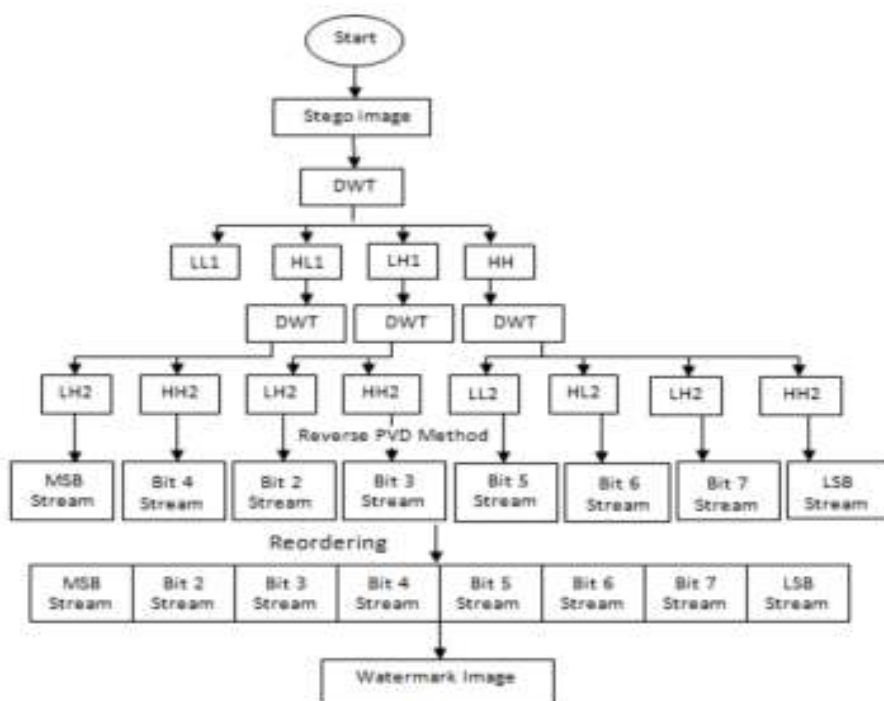


Fig. 21: The watermark recovery procedure

The first bits from each bit stream were gathered to retrieve the content of the first pixel of the watermark. The second bits of the bit stream were similarly gathered in order to recover the second pixel and so on until the entire content of the watermark signal/logo are recovered.

Experimental discussions presented in the next section ascertain the extent to which the proposed ordering combines with the PVD-based watermark embedding and extraction highlighted in this section to produce a better data hiding stratagem.

EXPERIMENTAL RESULTS AND DISCUSSION

To validate the veracity of the ordering proposed in the preceding sections, a dataset comprising 12 (cover or host) images (each of 256×256 pixel size) of varying visual complexity and labelled as Fingerprint, Baboon, Mountains.096, Flintstones, Buses.023, Couple, Lena, Boats, Dinosaurs.061, Elaine, Blood cells and Building,

which in that order are arranged according to their visual complexity as determined using the SND visual complexity space respectively (with complexity decreasing from left to right as we go downwards from the topmost row), were used as cover images on to which various sizes (110×110, 64×64 32×32 and 16×16) of the SAU logo watermark are hidden. The watermark embedding and extraction is carried out as detailed in the PVD-based system highlighted in above section.

Noteworthy from this dataset (Fig. 22) is the fact that the SND visual complexity space labels the popular Baboon and Lena images as being ‘complex’ images. This is mainly attributed to the edgy and highly textured nature of the images. The rest of this section is devoted to explanations about the experimental setup and analysis of the results obtained.

Compared alongside some recent data hiding techniques in Yaghmaee and Jamzad (2010) and Zhang *et al.* (2008), the proposed scheme exhibited appreciable performance in terms of both watermark embedding capacity and fidelity of the watermarked

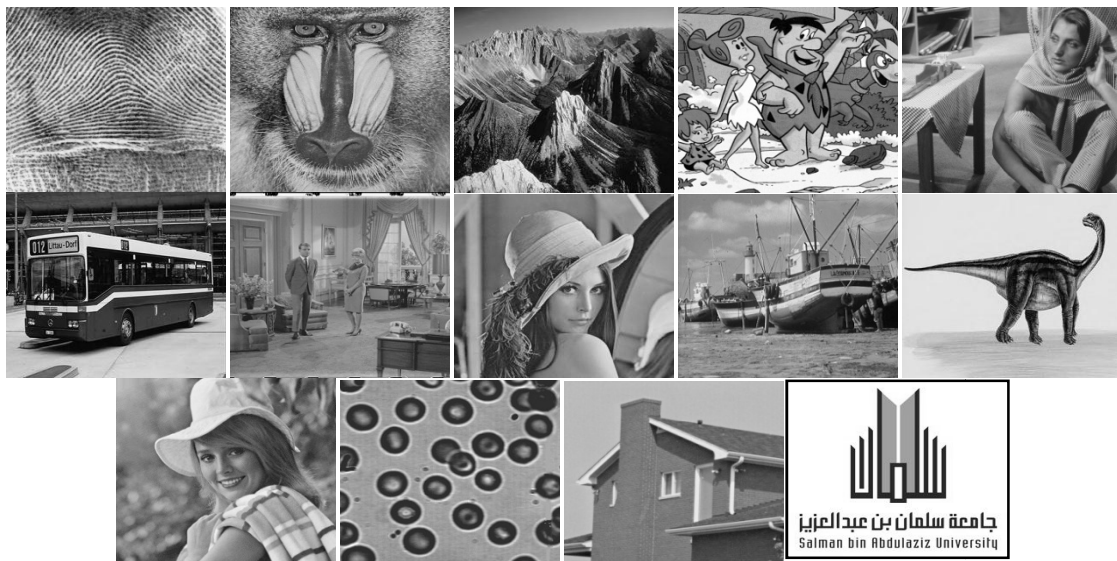


Fig. 22: Dataset showing the images (and the last image-the SAU watermark logo) used to evaluate the proposed scheme. The images are arranged according to their visual complexity as determined using the SND space (Le *et al.*, 2012)

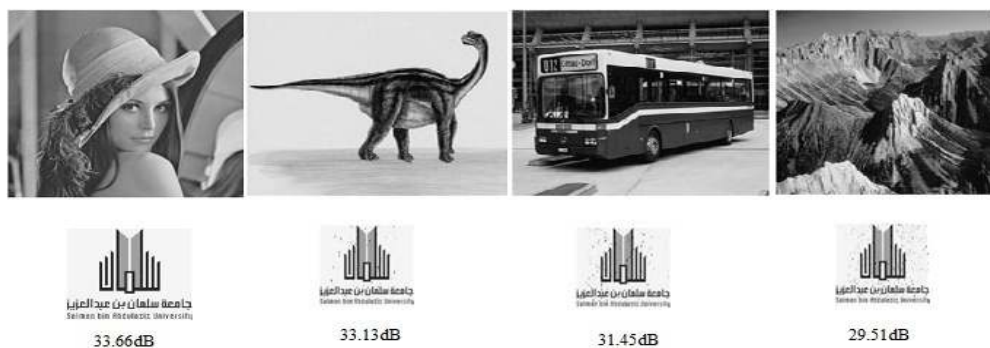


Fig. 23: Watermarked versions of 256×256 Lena, Dinosaur.061, Buses.023, and Mountains.096 host images; the 110×110 SAU watermark logos recovered from the watermarked images; and the PSNR values of the watermarked images

Table 3: PSNR values for different sizes of the SAU watermark logo

	Size of watermark/PSNR (in dB)			
	16×16	32×32	64×64	110×110
Cover image				
Lena	37.58	37.26	36.03	33.66
Dinosaurs.061 (simple)	36.90	36.60	35.41	33.13
Buses.023 (normal)	34.05	33.88	32.95	31.45
Mountains.096 (complex)	31.43	31.35	30.40	29.51

Table 4: Evaluation of watermarking capacity of the proposed method alongside some recent methods (Yaghmaee and Jamzad, 2010; Zhang *et al.*, 2008) (for 256×256 Lena image)

Method	Watermark capacity	
	Bits	PSNR (dB)
Zhang	80,599	31.80
Yaghmaee	73,896	N.A.
Proposed method	96,800	33.66

images represented by PSNR values as summarized in Table 3 for the Lena and 3 representative images (the Dinosaurs.061 for the 'simple' cluster, Buses.023 for the 'normal' cluster and Mountains.096 for the 'complex cluster').

Using these underpinnings, we conclude the section with an evaluation of the performance of the proposed data hiding technique alongside some recent watermarking methods.

Being the most widely used metric for comparing the fidelity of a watermarked image with its original version (Ilyasu *et al.*, 2012; Ilyasu, 2013a; Salama *et al.*, 2013), Peak-Signal-to-Noise Ratio (PSNR) will be used as our watermarked image quality evaluation metric.

Each of the cover images in our dataset was paired with SAU logo watermark. The resulting watermarked images, the recovered (extracted) watermark logo and PSNR values for the Lena and 3 representative images are presented in Fig. 23.

The evaluation of the visual quality of the watermarked versions of the Lena, Dinosaurs.061, Buses.023 and Mountains.096 images in our dataset (Fig. 22) using smaller sized versions (64×64, 32×32 and 16×16) of the SAU watermark logo are presented in Table 4. These results indicate an average PSNR of 37.58, 36.90, 34.05 and 31.43 dB, respectively for the 16×16 version of the SAU watermark logo that was embedded onto the Lena, Dinosaurs.061, Buses.023 and Mountains.096 images.

CONCLUSION

DWT decomposition of an image reveals a lot of information about such an image. Using a perspicacious analysis of this information, the best regions of a host image best suited to hide some secret data can be deduced. This study proposes a stratagem to accomplish that. In doing so, the most significant data from a watermark is hidden in the sub-bands of the DWT decomposed cover image that exhibit the least gain factor. This way, the visual quality and embedding

capacity of the watermarked image are enhanced. In addition, the proposal guarantees an efficient recovery of the hidden data. To determine the best ordering for hiding the data, various types of images of varying content and visual complexity were considered, analyzed and ranked in terms of their ability to withstand changes that do not imperil the visual quality (PSNR) of the watermarked image. Depending on this proposed ordering, an $N \times N$ -sized watermark stream is hidden in the 8 highest ranked sub-bands. The visual complexity classification of an image as simple, normal or complex of an image based on the structure, noise and diversity inherent to it was used to generalise an ordering of the DWT decomposed sub-bands of the image. Specifically, the MSBs from each pixel are then gathered and hidden in the best wavelet sub-band, the HLLH region, in order to enhance the robustness, while the LSBs are spread within the HHHH region. Finally, the remainder of the watermark stream is spread in the remaining 6 sub-bands of the host image in order to enhance the security of the data. Using the proposed strategy, a 256×256 Lena image had the capacity to accommodate 96800 bits of the SAU watermark logo while still maintaining an appreciable visual quality manifested by a PSNR value of 33.66 dB.

In on-going work, effort is being focussed on how to improve the SND visual complexity space so that it can be used to further enhance the quality of the data hiding techniques and other uses in image retrieval and computer vision.

ACKNOWLEDGMENT

This study was carried out with support from the Salman Bin Abdulaziz University via the Deanship for Scientific Research Special Research Grant No. 123/H/33.

REFERENCES

- Al-Asmari, A.K., M.A. Al-Qodah and A.S. Salama, 2011. Wavelet-pixel value differencing technique for digital images data hiding. Proceeding of the IEEE 2011 International Conference on System Engineering and Technology (ICSET), pp: 15-18.
- Al-Asmari, A.K., A.S. Salama, A.M. Ilyasu and M.A. Al-Qodah, 2012. A DWT ordering scheme for hiding data in images based on pixel value difference. Proceeding of the 8th International Conference on Computational Intelligence and Security (CIS). Ghoungou, China, pp: 553-557.
- Cardici, M., V.D. Gesu, M. Petrou and M.E. Tabacchi, 2009. A fuzzy approach to the evaluation of image complexity. Fuzzy Set. Syst., 60(10): 1474-1484.
- Cui, L. and L. Li, 2011. Adaptive multiwavelet-based watermarking through JPW masking. IEEE T. Image Process., 20(4): 1047-1060.

- Elbasi, E. and A.M. Eskicioglu, 2006. A semi-blind watermarking scheme for color images using a tree structure. Proceeding of the IEEE Sarnoff Symposium, Western New York Image Processing Workshop, Rochester Institute of Technology, Rochester, pp: 5-8.
- Griffin, G., A.D. Holub and P. Perona, 2013. The Caltech-256. Caltech Technical Report. Retrieved form: <http://www.vision.caltech.edu/ImageDatasets/Caltech256>, (Accessed on: Sept., 2013).
- Iliyasu, A.M., 2013a. Towards realising secure and efficient image and video processing applications on quantum computers. *Entropy*, 15(8): 2874-2974.
- Iliyasu, A.M., P.Q. Le, F. Dong and K. Hirota, 2012. Watermarking and authentication of quantum images based on restricted geometric transformations. *Inform. Sci.*, 186(1): 126-149.
- Iliyasu, A.M., A.K. Al-Asmari, M. Abdel Wahab, A.S. Salama, M.A. Al-Qodah, P.Q. Le and F. Yan, 2013b. Mining visual complexity of images based on an enhanced feature space representation. Proceeding of the 8th IEEE International Symposium on Intelligent Signal Processing (WISP 2013), pp: 65-70.
- Kim, J.R. and Y.S. Moon, 1999. A robust wavelet-based digital watermarking using level-adaptive thresholding. Proceeding of the IEEE International Conference on Image Processing (ICIP, 1999), 2: 226-230.
- Le, P.Q., A.M. Iliyasu, J.A.G. Sanchez, F. Dong and K. Hirota, 2011. A three dimensional feature space for representing visual complexity of images using their structure, noise and diversity. Proceeding of the 12th International Symposium on Advanced Intelligent Systems (ISIS, 2011), pp: 417-420.
- Le, P.Q., A.M. Iliyasu, J.A.G. Sanchez, F. Dong and K. Hirota, 2012. Representing visual complexity of images using a 3D feature space based on structure, noise and diversity. *J. Adv. Comput. Intell. Intell. Inform.*, 16(5): 631-637.
- Makhoghi, M., F. Akhlaghian and H. Danyali, 2010. Robust digital image watermarking using singular value decomposition. Proceeding of the IEEE International Symposium on Signal Processing and Information Technology (ISSPIT, 2010), pp: 219-224.
- Mario, M. Chacon, D. Alma and S. Corral, 2005. Image complexity measure: A human criterion free approach. Proceeding of Annual Meeting of the North American the Fuzzy Information Processing Society (NAFIPS, 2005), pp: 241-246.
- Rigau, J., M. Feixas and M. Sbert, 2005. An information-theoretic framework for image complexity. Proceedings of the 1st Eurographics Conference on Computational Aesthetics in Graphics Visualization and Imaging (Computational Aesthetics'05), pp: 177-184.
- Salama, A.S., R. Atta, R. Rizk and F. Waness, 2011. A robust digital image watermarking technique based on wavelet transform. Proceeding of the IEEE International Conference on System Engineering and Technology (ICSET), pp: 100-105.
- Salama, A.S., M.A. Al-Qodah, A.M. Iliyasu, A.K. Al-Asmari and F. Yan, 2013. A Hybrid Fusion Technique for Watermarking Digital Images. In: Świątek J. (Ed.), *Advances in Systems Science. Advances in Intelligent Systems and Computing*. Springer, DOI: 10.1007/978-3-319-01857-7_20, pp: 207-217.
- Tao, P. and A.M. Eskicioglu, 2004. A robust multiple watermarking scheme in the DWT domain, optics east. Proceeding of the Symposium on Internet Multimedia Management Systems V Conference. Philadelphia, pp: 133-144.
- Wang, X. and H. Zhao, 2006. A novel synchronization invariant audio watermarking scheme based on DWT and DCT. *IEEE T. Signal Process.*, 54: 12-22.
- Wang, C., X. Li and B. Yang, 2010. Efficient reversible image watermarking by using dynamical prediction-error expansion. Proceeding of the 17th IEEE International Conference on Image Processing (ICIP, 2010), pp: 3673-3676.
- Weng, S., Y. Zhao and J. Pan, 2008. A novel reversible data hiding scheme. *Int. J. Innov. Comput. I.*, 4(2): 351-358.
- Yaghmaee, F. and M. Jamzad, 2005. Computing watermark capacity in images according to their quad tree. Proceeding of the 5th IEEE International Symposium on Signal Processing and Information Technology, pp: 823-826.
- Yaghmaee, F. and M. Jamzad, 2010. Estimating watermarking capacity in gray scale images based on image complexity. *EURASIP J. Adv. Sig. Pr.*, 2010: 9. Article ID 851920, DOI: 10.1155/2010/851920.
- Zhang, F., X. Zhang and H. Zhang, 2008. Digital image watermarking capacity and detection error rate. *Pattern Recogn. Lett.*, 28: 1-10.